Published in final edited form as:
Arterioscler Thromb Vasc Biol. 2009 August ; 29(8): 1172–1178. doi:10.1161/ATVBAHA.109.185918.

Rapamycin inhibition of the Akt/mTOR pathway blocks select stages of VEGF-A^{164} driven angiogenesis, in part by blocking S6Kinase

Qi Xue, **Janice A. Nagy**, **Eleanor J. Manseau**, **Thuy L. Phung**, **Harold F. Dvorak***, and **Laura E. Benjamin***
All authors are members of the Center for Vascular Biology and the Department of Pathology at the Beth Israel Deaconess Medical Center, Harvard Medical School, Boston MA 02215

Abstract

Objective—We evaluated the stages of VEGF-A^{164} driven angiogenesis that are inhibited by therapeutic doses of rapamycin and the potential role of S6K1 in that response.

Methods and Results—We assessed the effects of rapamycin on the several stages of angiogensis and lymphangiogenesis induced with an adenovirus expressing VEGF-A^{164} (Ad-VEGF-A^{164}) in the ears of adult nude mice. Rapamycin (0.5mg/kg/day) effectively inhibited mTOR and downstream S6K1 signaling and partially inhibited Akt signaling, likely through effects on TORC2. The earliest stages of angiogenesis, including mother vessel formation and increased vascular permeability, were strikingly inhibited by rapamycin, as was subsequent formation of daughter glomeruloid microvasular proliferations. However, later stage formation of vascular malformations and lymphangiogenesis were unaffected. Retrovirally delivered isoforms and shRNAs demonstrated that S6K1 signaling plays an important role in early VEGF-A^{164}-angiogenesis.

Conclusions—Rapamycin potently inhibited early and mid stages of VEGF-A^{164} driven angiogenesis, but not late-stage angiogenesis or lymphangiogenesis. Rapamycin decreased phosphorylation of both Akt and S6, suggesting that both the TORC1 and TORC2 pathways are impacted. Inhibition of S6K1 signaling downstream of mTOR is a major component of rapamycin's anti-angiogenesis action.

Keywords

angiogenesis; VEGF-A; rapamycin; lymphangiogenesis

Introduction

The success of Avastin in treating vascular endothelial growth factor–A (VEGF-A) driven cancers and macular edema has demonstrated the potential clinical importance of anti-angiogenesis as a therapeutic approach [1]. Nonetheless, much remains to be learned about the steps and mechanisms by which VEGF-A induces the formation of new blood vessels and lymphatics [2, 3].

Correspondence should be addressed to L.E.B. at lbenjami@bidmc.harvard.edu.
*The senior authors contributed equally to this work

Disclosures
None

Rapamycin, an inhibitor of "mammalian target of rapamycin" (mTOR), is a natural macrolide antibiotic derived from *Streptomyces hygroscopicus*. It has been used for some years for immunosuppressing patients following organ transplantion [4] and recently it has shown potential in cancer therapy [5]. In addition to its likely role in inhibiting tumor cell growth, rapamycin has also been found to be anti-angiogenic [6], and we have shown that its effects on the tumor vasculature contributed importantly to its anti-cancer efficacy in a spontaneous mouse model of breast cancer [7].

The PI3K/Akt/mTOR pathway plays a central role in cell growth and metabolism, and rapamycin and related inhibitors have multiple effects on this pathway. Recently we demonstrated that, at low doses, rapamycin inhibits not only mTOR and downstream signaling, but also the Akt pathway upstream of mTOR [8]. This was puzzling but perhaps can be explained by the finding that mTOR is distributed in two discrete protein complexes, TORC1 and TORC2, only one of which, TORC1, binds rapamycin. In addition to mTOR, the TORC2 complex contains rictor, mLST8 and SIN1, and regulates Akt phosphorylation at S473 [9–12]. Some divergences in Akt downstream signaling have recently been found to depend on differences in the composition of TORC1 and TORC2. For example, although usually present in both TORC1 and TORC2, mLST8 is required for phosphorylation of the Akt-FOXO3 pathway, but not for the Akt-GSK3β (S9) or mTOR-S6K1 (S240/244) pathways [13]. Although TORC2 does not bind rapamycin, it has been thought that prolonged rapamycin treatment causes mTOR to be sequestered in TORC1 (its rapamycin binding complex), thus reducing the availability of mTOR for TORC2 assembly [10]. However, rapamycin also induces an early, transient rise in Akt signaling, perhaps via de-repression of IRS1, insulin receptor substrate 1, which potentiates PI3K signaling [14].

Studying a spontaneous mouse model of breast cancer, we recently reported that different cells and tissues responded with different levels of sensitivity to rapamycin's inhibitory effects on the Akt pathway [7]. Further, we found that, in general, tumor cells are more likely to maintain elevated Akt phosphorylation during prolonged rapamycin treatment, whereas Akt S473 phosphorylation was strongly inhibited in stromal cells [7]. However, because endothelial cells are particularly sensitive to rapamycin-mediated p-Akt S473 downregulation, we were not able to separate the effects of rapamycin on p-Akt S473 from its effects on mTOR downstream signaling, and particularly its effects on S6K1.

The current study had two goals: 1) Define the steps in VEGF-A driven angiogenesis and lymphangiogenesis that are rapamycin sensitive and 2) Determine whether S6K1 signaling plays a key role in the angiogeneic response to VEGF-A.

Materials and Methods

Animals and materials

4–6 weeks old female athymic Nu/Nu mice (NCI, Bethesda, MD) were used. Animal protocols were approved by the BIDMC IACUC. A nonreplicating adenoviral vector (Ad-VEGF-A^{164}) was engineered to express the predominant (164 aa) murine isoform of VEGF-A [3]. Recombinant human VEGF-A^{165} was from R&D Systems (Minneapolis, MN), rapamycin from Alexis Corporation (San Diego, CA). Antibodies were purchased as follows: anti-AKT, anti-phospho-AKT(Ser-473), anti-phospho-p70S6K(Thr-389), anti-S6, anti-phospho-S6 (Ser-240/244) and anti-HA-Tag from Cell Signaling Technology (Beverly, MA); anti-p70S6K1 from Santa Cruz Biotechnology (Santa Cruz, CA); anti-β-Actin from Sigma-Aldrich, Inc. (St. Louis, MO); anti-CD31 from BD Pharmingen (San Jose, CA); and anti-Lyve1 from Upstate (Temecula, CA).

Analysis of mouse ear vasculature

5×10^6 pfu of Ad-VEGF-A^{164} or LacZ were injected into mouse dorsal ear skin with a 30-gauge needle in 10 μl and treated with rapamycin i.p. as indicated. Ears were photographed as described (n = 12 mice) [3, 15]. Plasma leakage was measured with a double tracer method (six ear sites, 3 mice/group) [3]. Ear lymphatics were demonstrated by perfusion with colloidal carbon [15]. Lymphangiogenesis was quantified by measuring the fraction of total ear sections tissue occupied by lymphatics in Giemsa-stained 1μm sections [15] with NIH Image analysis software.

Immunohistochemistry

Immunohistochemistry for CD31, pAkt and pS6 were performed as previously described on paraformaldehyde fixed tissue [16]. For immunofluorescence, frozen sections were fixed in 4% paraformaldehyde, pH 7.4, for 5 min at room temperature, washed in PBS, blocked in 5% goat serum-0.1% Triton X-100 in PBS for 1 hour at room temperature. Sections were then incubated with primary antibodies to mouse anti-CD31 (1:100 dilution) and Rabbit Anti-Lyve-1 Polyclonal Secondary antibodies were diluted 1:200 in 5% goat serum in PBS.

Cell culture

Primary human umbilical vein endothelial cells (HUVECs) were from Clonetics. They were grown on plates coated with 30μg/ml Vitrogen (Cohesion, Palo Alto, CA) in EGM-MV Bullet Kit at 37°C, 5% CO_2. Passage 4–6 HUVEC at ~80% confluency were washed with PBS and serum-starved in 0.1% FBS in endothelial cell basic medium for 18h. Rapamycin was added for 1h prior to VEGF-A^{165} stimulation. 293T cells and NIH 3T3 cells were grown in Dulbecco's modified Eagle's medium with 10% fetal calf serum (FCS), 2 mM glutamine, penicillin (100 U/ml) and streptomycin (100 μg/ml).

Retroviral constructs and cell infection

A plasmid containing a constitutively active rapamycin-insensitive form of S6K1 (HA-S6K1-F5A-E3893A) was kindly provided by Dr. John Blenis [17]. It was subcloned into a pCMBP retroviral vector after digestion with *EcoR*I restriction; ends were blunted and digested with *Sal*I. After purification through LMP agarose, it was cloned into the pCMBP vector that was digested with *BamH*I, ends blunted and digested with *Xho*I. Retrovirus was generated using 293T cells and HUVEC were infected as described [18]. Briefly, 2 μg of target gene plasmid, 1.5 μg of pMD gag pol and 0.5 μg of pMD G were mixed, and transfected into 293T cells. Medium was changed after 16 h. The medium containing retrovirus was collected 48 h after transfection and used for infection into HUVEC after adding 10 μg/ml Polybrene. HUVEC were used for experiments 48 h after infection.

For S6K1-siRNA studies, we used recombinant pSUPER retro vector system (OligoEngine). The OligoEngine Workstation designed two gene-specific inserts with starting sites from 545 *GCAGTTAGAAAGAGAGGGA* (S6K1 siRNA #1) and from 1075 *AACTTCTGGCTCGAAAGGT* (S6K1 siRNA #2), which were separated by a 9-nucleotide non-complementary spacer (tctcttgaa) from the reverse complement of the same 19-nucleotide sequence. Non-targeting pSuper-control was constructed using a sequence *AAGAGGGAGGGAGACATAT*. These oligos were inserted into the pSUPER.retro.circular.vectors after digestion with *Bgl*II and *Hind*III. To make a siRNA pool, 1μg of each pSUPER vector (containing oligo 545 or 1075 inserts), 1.5 μg of pMD gag pol and 0.5 μg of pMD G were mixed and transfected into 293T cells to produce retroviruses as described above.

In vivo retrovirus studies

For preparation of retroviruses, culture medium from virus-producing 293T cells was passed through a 0.45μm syringe filter and centrifuged at 16,500 RPM, 4°C, for 2h, the pellet was resuspended in PBS and titered in NIH3T3 cells. For *in vivo* studies, mouse ears were injected with 5×10^6 pfu Ad-VEGF-A^{164} and 2d later with 10 μl each of retrovirus (5×10^8 pfu) in Polybrene (20 μg/ml).

Statistical Analysis

Quantitative data are expressed as mean ± SD or SEM. The unpaired Student's *t* test or Mann-Whitney test were used for statistical analysis.

Results

Initial experiments tested whether rapamycin would inhibit the angiogenic response induced by an adenoviral vector expressing VEGF-A^{164} (Ad-VEGF-A^{164}) [3]. This model has been extensively characterized and reproducibly induces, in sequence, new blood vessels of the several types that form in tumors and in healing wounds. Greatly enlarged, thin-walled, pericyte-poor, hyperpermeable mother vessels (MV) develop initially (1–5 days); subsequently these evolve into several types of daughter vessels, particularly glomeruloid microvascular proliferations (GMP) and vascular malformations (VM). Ad-VEGF-A^{164} also initiates lymphangiogenesis [15]. Hence, by selecting defined time windows for rapamycin treatment, we hoped to assess the impact of mTOR inhibition on successive stages of angiogenesis and on lymphangiogenesis.

Effects of rapamycin on the earliest stage of VEGF-induced angiogenesis (1–5 days)

Intradermal injection of 5×10^6 pfu of Ad-VEGF-A^{164} into nude mouse ears induced the expected, robust angiogenic response. Treatment with rapamycin, beginning 24h prior to Ad-VEGF-A^{164} injection, inhibited angiogenesis in a dose-dependent manner (Fig. 1A). Ad-lacZ served as a negative control. To document the efficacy of rapamycin on mTOR inhibition, we collected 8mm punch biopsies of the ear reaction sites on day 5 for immunoblotting to assess expression and phosphorylation of S6 and Akt (Fig. 1B). Rapamycin potently inhibited phosphorylation of S6 (downstream of S6K) in a dose-dependent manner. As previously shown [8], p-Akt (S473) was somewhat reduced.

We recently made a careful study of the doses of rapamycin in mice that achieve the clinically recommended blood levels of rapamycin used for treating human transplant recipients [7]. We found that the relatively low dose of 0.5mg/kg/day resulted in the 10–20ng/mL trough plasma levels of rapamycin desired clinically. This low dose of rapamycin partially inhibited angiogenesis (Fig. 1A), and reduced plasma leakage by ~60% (Fig. 1C), an impressive feat in that Ad-VEGF-A^{164} generates high, tumor-like concentrations of VEGF-A^{164} (up to 120 ng/8 mm punch site at 24h) [3]. Associated tissue edema, assessed by ear thickness, was also strikingly reduced, as were the number of new MV that formed (Fig. 1D, left panel).

Immunohistochemistry with antibodies specific for the phosphorylated forms of S6 (S240/244) and Akt (S473) were used to assess rapamycin's effects on cell signaling. MV staining for p-S6 was strikingly reduced, while p-Akt staining was less affected (Fig. 1D, right panels). Of interest, lymphatic vessels in mice injected with Ad-VEGF-A^{164} alone did not stain strongly for p-Akt, even though the endothelial cells lining these vessels were actively proliferating [15] (Fig. 1D).

Effects of rapamycin on MV evolution into daughter vessels and on lymphangiogenesis (days 5–12)

By 5 days after injection of Ad-VEGF-A^{164}, tissue levels of VEGF-A-^{164} have fallen ~ 10-fold from those at 1 day and new MV formation has ceased [2]. Over the course of the following week, MV that had already formed differentiated into daughter glomeruloid microvascular proliferations (GMP) and vascular malformations (VM). In addition, a robust lymphangiogenic response developed, leading to the formation of large numbers of abnormally enlarged "giant" lymphatics [15]. To assess the effects of rapamycin on this stage of VEGF-A-^{164}-driven angiogenesis and lymphangiogenesis, we began treatment on day 5 after Ad-VEGF-A^{164} administration and continued it daily until harvesting ears on day 12. Rapamycin dramatically reduced overall vascularity by day 12 (Fig. 2A) and strikingly reduced the numbers and size of GMP (Figs. 2B,C), but did not noticeably affect VM formation. GMP stained strongly for both p-Akt and p-S6 in mice receiving Ad-VEGF-A-^{164} alone, whereas, in rapamycin-treated mice, the few, poorly formed GMP that developed stained weakly for p-Akt and even more weakly for p-S6.

To assess the effects of rapamycin on VEGF-A^{164}-induced lymphangiogenesis, we performed intravital perfusion of the lymphatics in mouse ears with colloidal carbon. Fig. 3A illustrates the ears shown in Fig. 2A following such perfusion; rapamycin at a dose of 0.5 mg/kg/day had little or no effect on the new VEGF-A^{164}-induced lymphatic network. Consistently, immunofluorescent double staining (Fig. 3B) demonstrated that rapamycin-treated ears had many fewer CD31-stained blood vessels but not fewer Lyve-1-positive lymphatic vessels. Quantification of the lymphatic response is shown in Fig. 3C.

Effects of rapamycin on late stages of VEGF-induced angiogenesis (days 35–49)

VEGF-A-^{164}-driven angiogenesis culminates in the formation of VM, essentially MV that have acquired an irregular coat of smooth muscle cells [2]. Unlike MV and GMP, VM, once formed, persist indefinitely (>1year); the giant lymphatics induced by Ad-VEGF-A^{164} also persist indefinitely. To test the effects of rapamycin on these vessels, we began treatment at 35 days after injection of Ad-VEGF-A^{164} and continued it daily until day 49. Because we have not observed any complications of rapamycin treatment in otherwise mature and normal vascular beds, we were surprised to find macroscopic evidence of vascular changes at this late stage (Fig. 4A, day 49, note intense, focal redness). Histology revealed that VM formation was not diminished in rapamycin-treated mice. However, a number of VM in rapamycin-treated mice had thrombosed and were filled with platelet- and fibrin-rich blood clots (Fig. 4B). As at earlier times, lymphatics in ears injected with Ad-VEGF-A^{164} (here containing colloidal carbon following intralymphatic injection) did not stain detectably with antibodies against p-Akt and p-S6 (Fig. 4B).

Finally, we performed Western blots to assess p-Akt and p-S6 activity over the entire time course of our experiments. As shown in Fig. 4C, the intensity of both p-Akt and p-S6 bands declined gradually over time from peak values at day 5 in the ears of untreated mice. In rapamycin treated mice, p-S6 bands were strikingly reduced, in comparison with comparable controls, at all time points; p-Akt bands were also reduced, but to a lesser extent.

Effects of constitutively active S6K1 and S6K1-specific shRNAs on Ad-VEGF-A^{164}-induced angiogenesis

Rapamycin strongly inhibits S6K1 phosphorylation of S6 but also has a minor effect on Akt phosphorylation. Therefore, to test the effects of S6K1 inhibition independent of concomitant changes on Akt signaling, we prepared retroviruses that expressed either a constitutively active S6K1 or S6K1-specific shRNAs and determined their effects on Ad-VEGF-A^{164}-induced angiogenesis. We first tested these retroviruses on HUVEC (Fig. 5A). Constitutively activated

S6K1 expression was monitored by its HA tag and by increased phosphorylation of S6K1 at threonine 389, the rapamycin-sensitive residue (Fig. 5A). As expected, rapamycin did not inhibit phosphorylation of SK61 at T389 in cells expressing the constitutively active S6K1 since this isoform is mTOR independent. These cells also did not exhibit any change in p-Akt expression. HUVEC were also infected with retroviruses expressing S6K1-specific shRNAs. When silenced with either of two independent shRNAs, or by the two shRNAs pooled, total and phosphorylated S6K1 levels were strikingly reduced (Fig. 5B). Total Akt was not changed but p-AktS473 may have increased slightly. A similar finding has been reported previously and was proposed to reflect de-repression of IRS-1 [14].

We next injected these retroviruses into the ears of mice that had been injected 2d previously with Ad-VEGF-A^{164}. We chose this time because endothelial cells have begun to divide rapidly at this time and retroviruses only stably integrate into proliferating cells. As shown in Fig. 5C, ears injected with retroviruses expressing constitutively active S6K1 showed an enhanced angiogenic response at day 5, above that induced by Ad-VEGF-A^{164} alone; this response was slightly reduced by rapamycin, likely because not all endothelial cells are infected by the retrovirus. Ears injected with an S6K1 silencing retrovirus exhibited a reduced angiogenic response (Fig. 5C).

Supplemental Fig. 1A shows the histology of these ears at 5d. Large numbers of typical MV were found in mice injected with Ad-VEGF-A^{164} and also in those injected with a retrovirus expressing constitutively active S6K. Rapamycin had little inhibitory effect on MV formation in the presence of the constitutively active S6K1, compared to its dramatic inhibition of MV formation in ears injected with Ad-VEGF-A^{164} alone (compare with Figs. 1A,D). However, injecting Ad-VEGF-A^{164} infected ears with an S6K1 silencing retrovirus substantially reduced the number and size of MV that formed (Sup.Fig. IA, right panel). Immunohistochemistry demonstrated strong p-S6 reactivity in the great majority of MV endothelial cells induced by Ad-VEGF-A^{164} alone and also in those also injected with a retrovirus expressing active S6K1; in the latter mice, some endothelial cells, presumably those not infected with the retrovirus expressing activated S6K1, exhibited reduced staining as the result of rapamycin repression. Injection of the retrovirus expressing the shRNA silencing S6K1 showed greatly reduced MV p-S6 and slightly increased p-Akt staining. Together the histology demonstrates that S6K1 has a critical role in VEGF-A^{164}-induced MV induction.

This conclusion was further substantiated by immunoblots of whole ear reaction site lysates (Supplemental Fig. IB). S6K1 and p-S6 were increased in the Ad-VEGF-A^{164} injection sites of ears that were also injected with retrovirus-expressing S6K1, but p-Akt and total Akt were unchanged. Rapamycin treatment reduced p-S6 in these ears and to a lesser extent p-Akt. When Ad-VEGF-A^{164} injection sites were injected 2d later with retroviruses expressing either of two shRNAs that silence S6K1, or with a combination of the two shRNAs, p-S6 was strikingly reduced whereas p-Akt was modestly increased.

Discussion

In this study we examined the effects of rapamycin on VEGF-A^{164}-induced angiogenesis and lymphangiogensis. Previous studies using tumor models were limited by their inability to dissect apart the effects of rapamycin on tumor versus stromal cells. The adenoviral model offers the added advantage that different types of vessels form sequentially in a temporally defined manner; thus, the angiogenic response can be studied at discrete early, mid, and late stages, each involving different types of blood vessels. Using this model, we made several novel observations. First, the Akt and S6K1 signaling pathways are differentially upregulated during this response. At early times, MV highly expressed both Akt and S6K1 signaling. At middle times, it was proliferating GMP that were active, and at later stages, VM. However,

VEGF-A^{164}-induced lymphatics exhibited relatively little Akt and S6 phosphorylation. The inhibitory effects of rapamycin consistently matched the stages of highest p-Akt expression, and VEGF-A^{164}-induced lymphatics were insensitive to rapamycin. The VEGF-A^{164} levels induced in our adenovirus model are high and formation of new vessels could not be completely suppressed by low dose (0.5mg/kg/day) rapamcyin, compared with higher doses (Fig. 1A). Nonetheless, the 0.5mg/kg/day dose provides plasma levels of rapamycin that are clinically relevant. Therefore, they allowed us to determine which VEGF-A^{164}-driven vessel subtypes are most sensitive to rapamycin and are useful for translating our findings to patients receiving rapamycin treatment. In studies of rapamycin's anti-angiogenic activity, several laboratories have demonstrated that rapamycin has anti-cancer efficacy [8, 19, 20]. Moreover, a relatively tumor-specific thrombosis of blood vessels has been correlated to changes in endothelial expression of tissue factor [19].

Using the Ad-VEGF-A^{164} model combined with retrovirally-delivered dominant active and loss-of-function S6K1 isoforms, we were able to demonstrate the importance of S6K1 signaling at least in the early and mid-stages of VEGF-A^{164} driven angiogenesis and separated that requirement from overall Akt signaling. As Akt has multiple downstream targets that lead to pathways other than mTOR and S6K, this finding clarifies the importance of S6K1 downstream of Akt signaling in the overall angiogenic response. Earlier studies with rapamycin could not definitively make this conclusion because of the feedback on Akt. Given that we did not observe a reduction in p-Akt in cells overexpressing the dominant active S6K1 (Fig. 5A), or by immunohistochemistry (Supp Fig. 1A), or in whole lysates (Supp Fig. 1B), we conclude that the observed reduction in angiogenesis when we silence S6K1 is not via feedback inhibition of p-Akt, as we find with rapamycin, and supports the conclusion that S6K1 itself is essential for VEGF-A^{164}-driven angiogenesis. If anything, as we also observed in cell culture, there is a slight increase in p-Akt in the ear model when S6K1 is silenced. While we did not test silencing of S6K1 at later stages of VEGF-A^{164}-driven angiogenesis, extrapolating our findings suggests that later stages that are rapamycin-sensitive, such as GMP formation, will have a similar dependency on S6K. We also predict that vessels with low expression of phosphorylated S6, such as lymphatics and VM, will have less sensitivity to S6K1 inhibition, as they do to rapamycin treatment.

The late stage of VEGF-A^{164}-induced angiogenesis (35–49d) was confounding in that local increases in p-Akt were observed in response to rapamycin, but in the absence of altered p-S6 expression. This suggests that rapamycin is inducing a different response in these vessels and may have a role in inducing the thrombosis observed in VM. Taken together, it is clear that the vascular response to rapamycin is heterogeneous and that different vessel subtypes are differentially affected. The thrombosis observed in VM could be of clinical concern if in fact rapamycin induces vascular thrombosis. However, further investigation will be necessary to assess whether VM thrombosis within tumors is a risk or, possibly, a benefit to cancer patients.

A final surprise was the lack of p-Akt and p-S6 expression in lymphatics. This is in contrast to reports in other models and may reflect a difference between the lymphangiogenesis induced by VEGF-A^{164} through VEGFR2 versus that induced by other stimuli such as VEGF-C through VEGFR3 [21–23]. Future studies are required to determine the explanation for the difference in signaling in our Ad-VEGF-A induced lymphatics and those induced by other means. A recent report showed that although VEGF isoforms that only bind VEGFR2 are capable of inducing lymphangiogenesis, they cannot rescue loss of lymphatics due to inhibition of VEGFR3, further supporting the notion that VEGF-A^{164}-driven lymphangiogenesis may be wholly independent of VEGFR3 signaling [24]. This also suggests that the new lymphatics induced by VEGF-A^{164} can remain functional in reducing edema and clearing waste products even while VEGFA^{164}-driven angiogenesis is inhibited by rapamycin.

Supplementary Material

Refer to Web version on PubMed Central for supplementary material.

Acknowledgements

Thanks to H. Zeng and D. Zhao for help in retroviral cloning of shRNA and transduction of HUVEC.

Sources of Funding

Funding: P01 CA092644 to H.F.D. and L.E.B. R01's CA131064 & HL1049 to L.E.B. RO1 HL 64402 and a contract from the National Foundation for Cancer Research to H.F.D.

References

1. Jain RK. Lessons from multidisciplinary translational trials on anti-angiogenic therapy of cancer. Nat Rev Cancer 2008;8:309–316. [PubMed: 18337733]
2. Nagy JA, Dvorak AM, Dvorak HF. VEGF-A and the Induction of Pathological Angiogenesis. Annu Rev Pathol 2007;2:251–275. [PubMed: 18039100]
3. Nagy JA, Shih SC, Wong WH, Dvorak AM, Dvorak HF. Chapter 3. The adenoviral vector angiogenesis/lymphangiogenesis assay. Methods Enzymol 2008;444:43–64. [PubMed: 19007660]
4. Motzer RJ, Escudier B, Oudard S, Hutson TE, Porta C, Bracarda S, Grunwald V, Thompson JA, Figlin RA, Hollaender N, Urbanowitz G, Berg WJ, Kay A, Lebwohl D, Ravaud A. Efficacy of everolimus in advanced renal cell carcinoma: a double-blind, randomised, placebo-controlled phase III trial. Lancet 2008;372:449–456. [PubMed: 18653228]
5. Knox JJ. Progression-free survival as endpoint in metastatic RCC? Lancet 2008;372:427–429. [PubMed: 18653227]
6. Guba M, von Breitenbuch P, Steinbauer M, Koehl G, Flegel S, Hornung M, Bruns CJ, Zuelke C, Farkas S, Anthuber M, Jauch KW, Geissler EK. Rapamycin inhibits primary and metastatic tumor growth by anti-angiogenesis: involvement of vascular endothelial growth factor. Nat Med 2002;8:128–135. [PubMed: 11821896]
7. Phung TL, Eyiah-Mensah G, O'Donnell RK, Bieniek R, Shechter S, Walsh K, Kuperwasser C, Benjamin LE. Endothelial Akt signaling is rate-limiting for rapamycin inhibition of mouse mammary tumor progression. Cancer Res 2007;67:5070–5075. [PubMed: 17545582]
8. Phung TL, Ziv K, Dabydeen D, Eyiah-Mensah G, Riveros M, Perruzzi C, Sun J, Monahan-Earley RA, Shiojima I, Nagy JA, Lin MI, Walsh K, Dvorak AM, Briscoe DM, Neeman M, Sessa WC, Dvorak HF, Benjamin LE. Pathological angiogenesis is induced by sustained Akt signaling and inhibited by rapamycin. Cancer Cell 2006;10:159–170. [PubMed: 16904613]
9. Sarbassov dos D, Guertin DA, Ali SM, Sabatini DM. Phosphorylation and regulation of Akt/PKB by the rictor-mTOR complex. Science 2005;307:1098–1101. [PubMed: 15718470]
10. Sarbassov dos D, Ali SM, Sengupta S, Sheen JH, Hsu PP, Bagley AF, Markhard AL, Sabatini DM. Prolonged rapamycin treatment inhibits mTORC2 assembly and Akt/PKB. Mol Cell 2006;22:159–168. [PubMed: 16603397]
11. Jacinto E, Facchinetti V, Liu D, Soto N, Wei S, Jung SY, Huang Q, Qin J, Su B. SIN1/MIP1 maintains rictor-mTOR complex integrity and regulates Akt phosphorylation and substrate specificity. Cell 2006;127:125–137. [PubMed: 16962653]
12. Yang Q, Inoki K, Ikenoue T, Guan KL. Identification of Sin1 as an essential TORC2 component required for complex formation and kinase activity. Genes Dev 2006;20:2820–2832. [PubMed: 17043309]
13. Guertin DA, Stevens DM, Thoreen CC, Burds AA, Kalaany NY, Moffat J, Brown M, Fitzgerald KJ, Sabatini DM. Ablation in mice of the mTORC components raptor, rictor, or mLST8 reveals that mTORC2 is required for signaling to Akt-FOXO and PKCalpha, but not S6K1. Dev Cell 2006;11:859–871. [PubMed: 17141160]

14. O'Reilly KE, Rojo F, She QB, Solit D, Mills GB, Smith D, Lane H, Hofmann F, Hicklin DJ, Ludwig DL, Baselga J, Rosen N. mTOR inhibition induces upstream receptor tyrosine kinase signaling and activates Akt. Cancer Res 2006;66:1500–1508. [PubMed: 16452206]
15. Nagy JA, Vasile E, Feng D, Sundberg C, Brown LF, Detmar MJ, Lawitts JA, Benjamin L, Tan X, Manseau EJ, Dvorak AM, Dvorak HF. Vascular permeability factor/vascular endothelial growth factor induces lymphangiogenesis as well as angiogenesis. J Exp Med 2002;196:1497–1506. [PubMed: 12461084]
16. Xue Q, Hopkins B, Perruzzi C, Udayakumar D, Sherris D, Benjamin LE. Palomid 529, a novel small-molecule drug, is a TORC1/TORC2 inhibitor that reduces tumor growth, tumor angiogenesis, and vascular permeability. Cancer Res 2008;68:9551–9557. [PubMed: 19010932]
17. Schalm SS, Tee AR, Blenis J. Characterization of a conserved C-terminal motif (RSPRR) in ribosomal protein S6 kinase 1 required for its mammalian target of rapamycin-dependent regulation. J Biol Chem 2005;280:11101–11106. [PubMed: 15659381]
18. Zeng H, Zhao D, Yang S, Datta K, Mukhopadhyay D. Heterotrimeric G alpha q/G alpha 11 proteins function upstream of vascular endothelial growth factor (VEGF) receptor-2 (KDR) phosphorylation in vascular permeability factor/VEGF signaling. J Biol Chem 2003;278:20738–20745. [PubMed: 12670961]
19. Guba M, Yezhelyev M, Eichhorn ME, Schmid G, Ischenko I, Papyan A, Graeb C, Seeliger H, Geissler EK, Jauch KW, Bruns CJ. Rapamycin induces tumor-specific thrombosis via tissue factor in the presence of VEGF. Blood 2005;105:4463–4469. [PubMed: 15671443]
20. Stephan S, Datta K, Wang E, Li J, Brekken RA, Parangi S, Thorpe PE, Mukhopadhyay D. Effect of rapamycin alone and in combination with antiangiogenesis therapy in an orthotopic model of human pancreatic cancer. Clin Cancer Res 2004;10:6993–7000. [PubMed: 15501979]
21. Kobayashi S, Kishimoto T, Kamata S, Otsuka M, Miyazaki M, Ishikura H. Rapamycin, a specific inhibitor of the mammalian target of rapamycin, suppresses lymphangiogenesis and lymphatic metastasis. Cancer Sci 2007;98:726–733. [PubMed: 17425689]
22. Matsuo M, Yamada S, Koizumi K, Sakurai H, Saiki I. Tumour-derived fibroblast growth factor-2 exerts lymphangiogenic effects through Akt/mTOR/p70S6kinase pathway in rat lymphatic endothelial cells. Eur J Cancer 2007;43:1748–1754. [PubMed: 17570654]
23. Salameh A, Galvagni F, Bardelli M, Bussolino F, Oliviero S. Direct recruitment of CRK and GRB2 to VEGFR-3 induces proliferation, migration, and survival of endothelial cells through the activation of ERK, AKT, and JNK pathways. Blood 2005;106:3423–3431. [PubMed: 16076871]
24. Wirzenius M, Tammela T, Uutela M, He Y, Odorisio T, Zambruno G, Nagy JA, Dvorak HF, Yla-Herttuala S, Shibuya M, Alitalo K. Distinct vascular endothelial growth factor signals for lymphatic vessel enlargement and sprouting. J Exp Med 2007;204:1431–1440. [PubMed: 17535974]

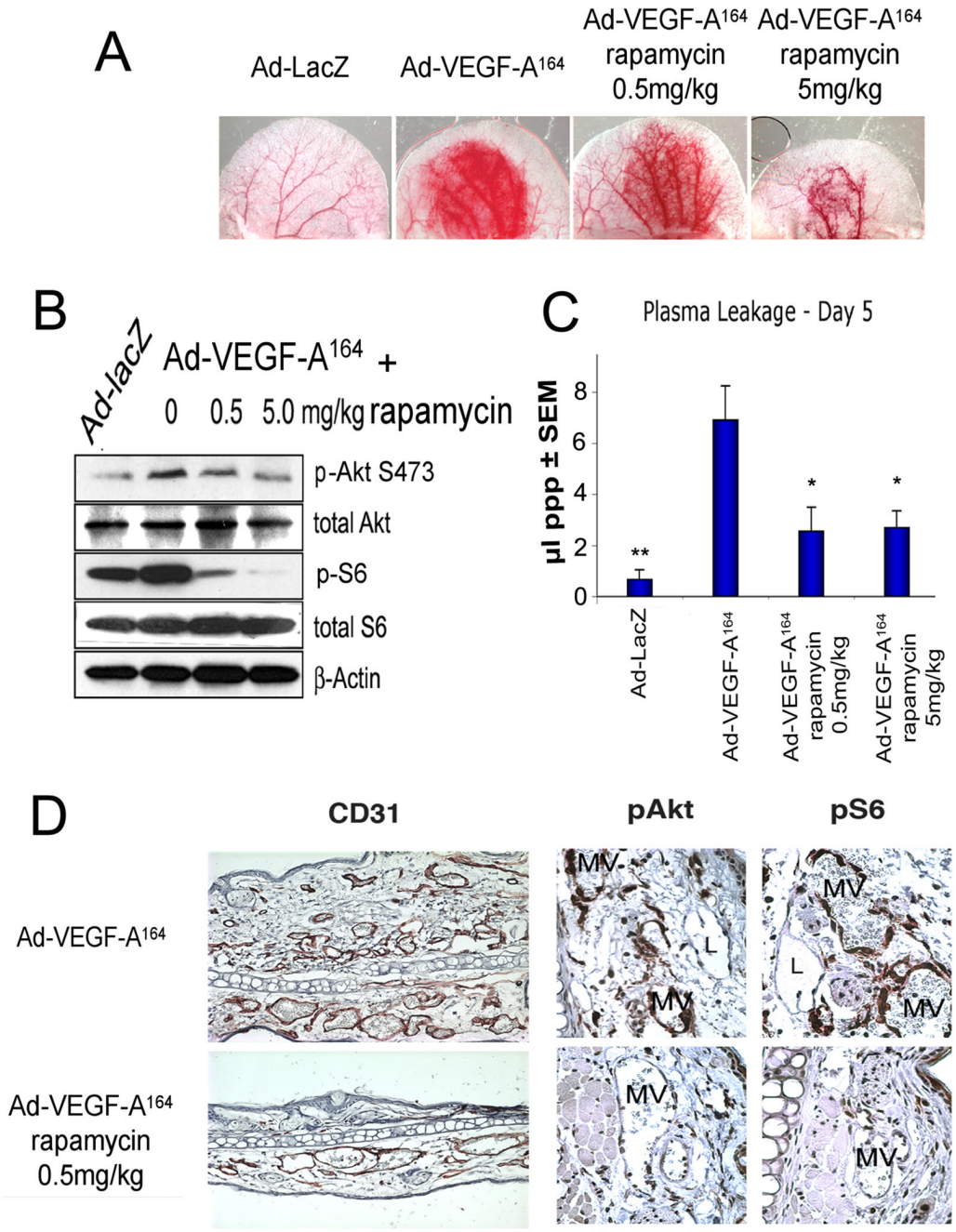

Figure 1. Effects of rapamycin on early, 5 day angiogenic response induced by Ad-VEGF-A^{164} in mouse ears

Mice were treated daily with 0, 0.5 or 5mg/kg rapamycin, starting 1d before 5×10^6 pfu Ad-VEGF-A^{164} injection. Ad-lacZ, control. (**A**) Ears at 5d (×8). (**B**) Immunoblot of lysates of ear angiogenic sites removed with an 8mm punch. (**C**) Volume of extravasted plasma in control and rapamycin-treated sites as a quantitative measure of vascular permeability **P<0.01, *P<0.05 versus Ad-VEGF-A^{164} using Mann-Whitney test. (**D**) Immunohistochemical staining for CD31 (left panel) and for p-Akt and p-S6 (middle and right panels) in ears injected with Ad-VEGF-A^{164} ± 0.5mg/kg rapamycin. MV, mother vessels, L, lymphatics.

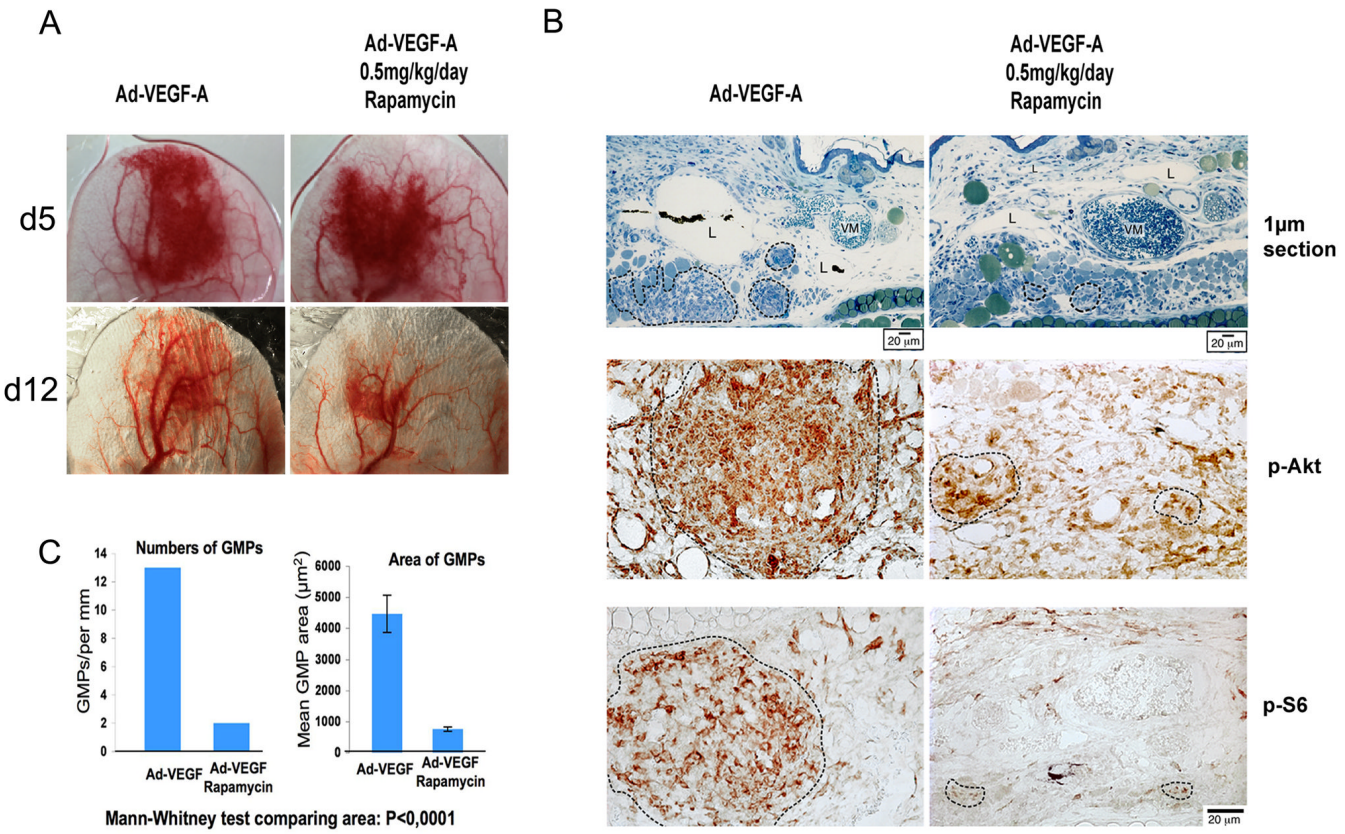

Figure 2. Low dose rapamycin inhibits VEGF-A-induced formation of GMP, but not VM

Mice were treated with 0.5 mg/kg rapamycin daily from 5–12d after Ad-VEGF-A^{164} injection. (**A**) Ears on 5 and 12d. **(B)** Top panel: Giemsa-stained 1µm sections of ears at 12d after Ad-VEGF-A^{164}. Note giant lymphatics (L, some containing colloidal carbon), greatly reduced GMP, but unchanged VM in rapamycin-treated mice. Lower panels: Strong immunostaininig of GMP for both p-Akt and p-S6 in controls; however, the few GMP that formed in rapamycin-treated mice stained weakly or not at all. Dotted lines outline GMP. Magnification bar, 20 µm. (**C**) Morphometric analysis of 1µm sections, quantifying the number and size of GMP at 12d following Ad-VEGF-A^{164} injection ± rapamycin. Statistical analysis was done with an unpaired student's t test.

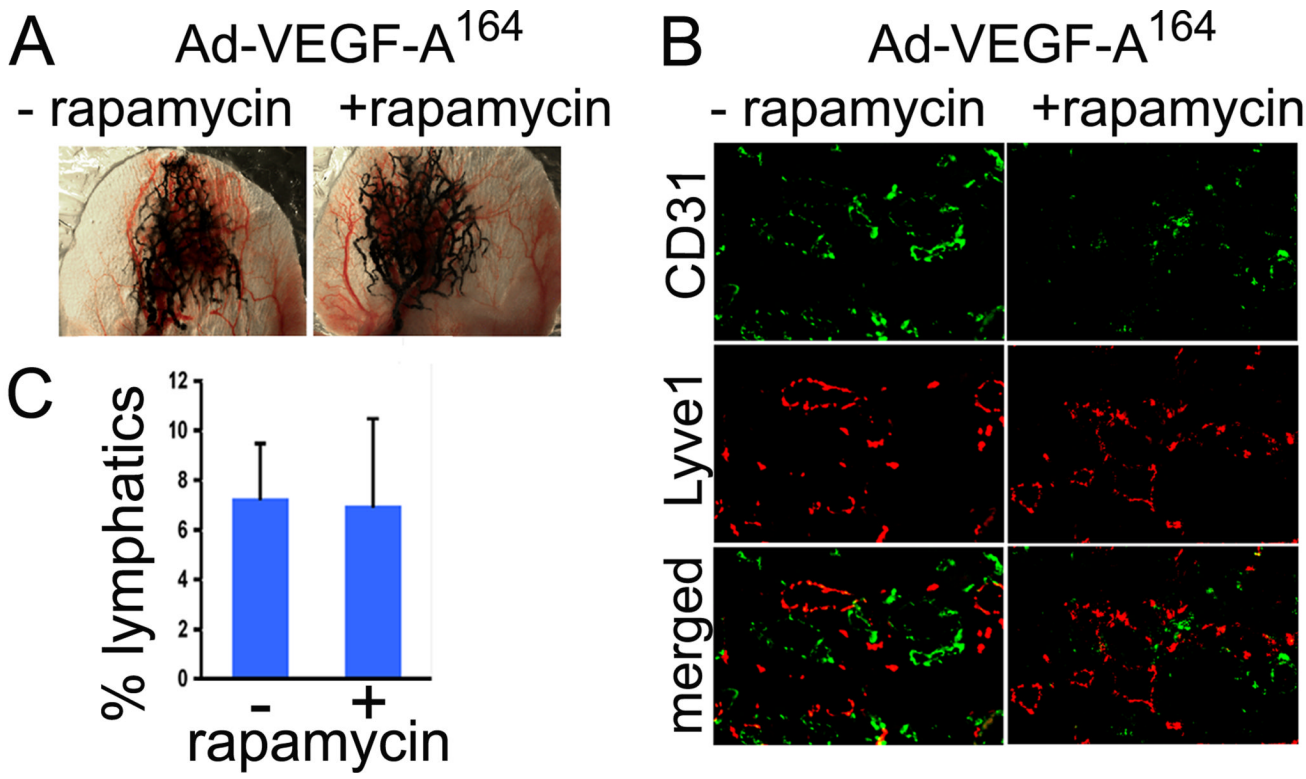

Figure 3. Rapamycin does not affect Ad-VEGF-A^{164}-induced lymphatics

Mice were treated with 0.5mg/kg rapamycin daily from 5 –12d after injection of Ad-VEGF-A^{164}. (**A**) 12d ears after injection of colloidal carbon into the lymphatic network. (**B**) Immunofluorencent double staining for CD31 (green) and Lyve1 (red) in 12d ears. **(C)** Morphometric analysis of lymphatics in 1μm sections of ears injected with Ad-VEGF-A^{164} 12d previously ± rapamycin.

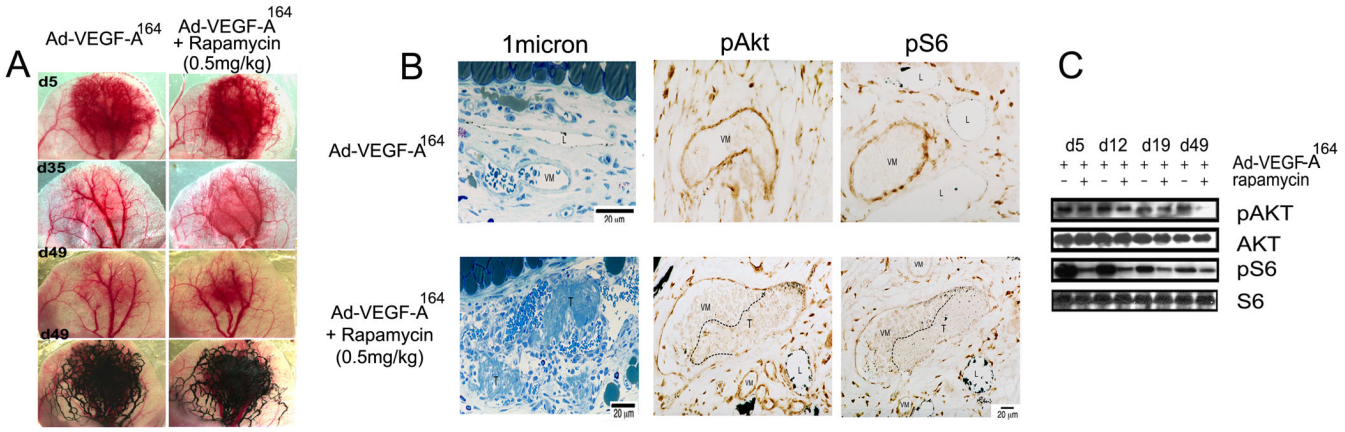

Figure 4. Effects of rapamycin on blood and lymphatic vessels at late stages after Ad-VEGF-A^{164} injection

Mice were treated with 0.5mg/kg rapamycin daily from 35 – 49d after Ad-VEGF-A^{164} injection. (**A**) Ears at 5, 35 and 49d after Ad-VEGF-A^{164} injection. Two lower panels show representative mouse ears at 49d, before and after intravital perfusion of colloidal carbon into the lymphatic network. (**B**) Histology at 49 days assessed by 1μm sections. Note thrombosis (T) in VM of rapamycin-treated mice. L, lymphatics. Right panels illustrate p-AKT and p-S6 immunostaining. Dotted lines outline thrombi (T). Magnification bar, 20 μm. (**C**) Immunoblot analyzing p-Akt and p-S6 in control and rapamycin (0.5mg/kg/day)-treated ear lysates at indicated times after Ad-VEGF-A^{164} injection.

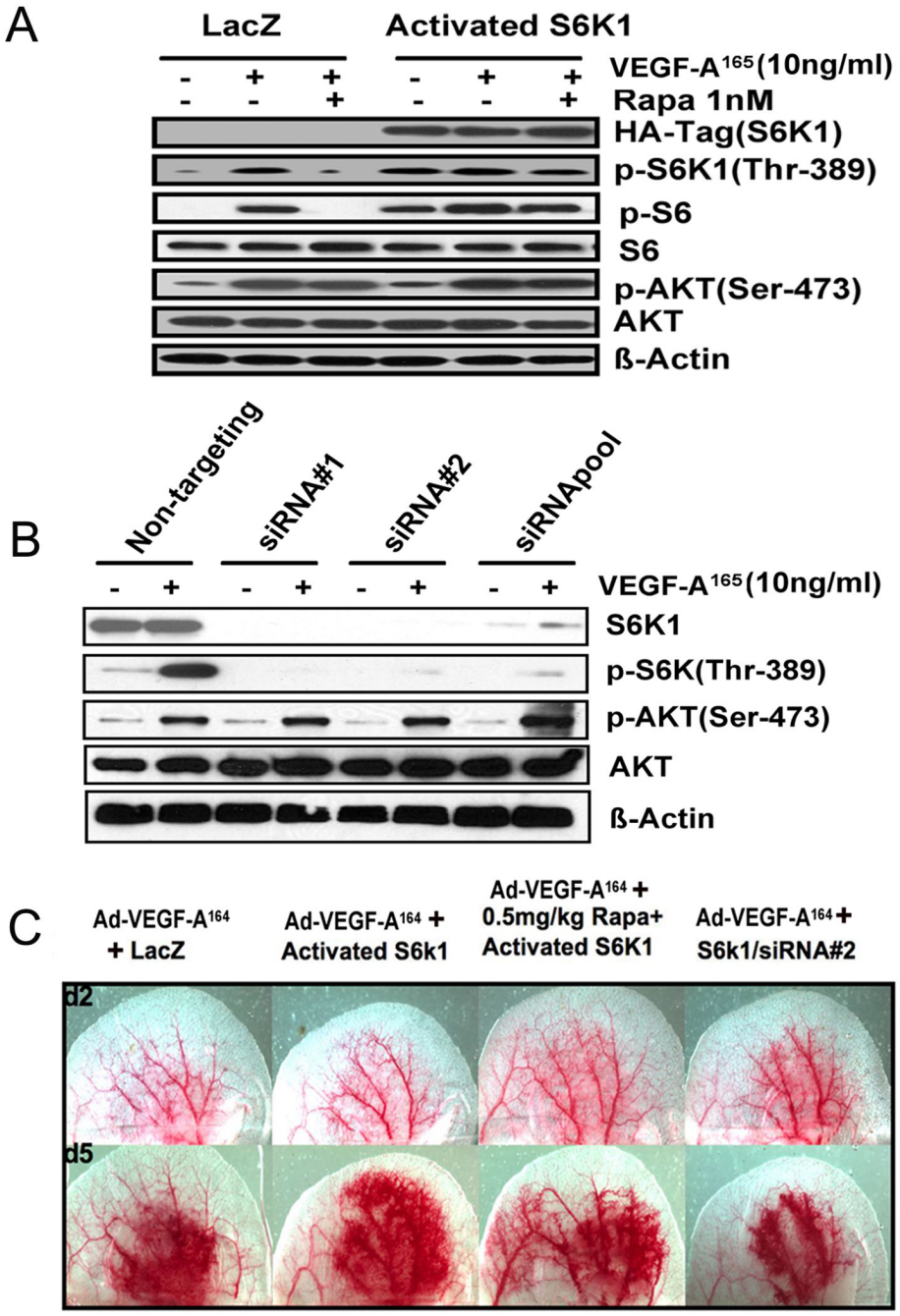

Figure 5. Role of S6K1 signaling in VEGF-A-induced angiogenesis

(**A**) Immunoblot of HUVEC lysates that had been infected with retroviruses expressing either an activated isoform of S6K1 or LacZ. After 18 h of serum starvation, cells were stimulated with human VEGF-A^{165} (10ng/ml, 10 min) ± pre-treatment for 1h with 1 nM rapamycin. (**B**) Immunoblot of HUVEC lysates that had been infected with retroviruses expressing S6K1 shRNAs or a non-targeting shRNA. After serum-starvation for 18h, cells were stimulated with VEGF-A^{165} (10ng/ml, 10 min). Results are representative of three independent experiments. (**C**) Mouse ears were injected with 5×10^8 PFU of Ad-VEGF-A^{164}. Two days later, the same ear sites were injected with retroviruses expressing the activated form of S6K1 or with an S6K1 shRNA, as indicated. Rapamycin (0.5mg/kg/day) treatment was begun 1 day before injection

of Ad-VEGF-A^{164}. Ears were photographed at 2d (prior to injection of retroviruses, top panel), and 5d (bottom panel).